

The monitoring of progress in apoptosis of liver cells in bile duct-ligated rats

Safra yolu bağlanan sıçanlarda karaciğer hücrelerindeki apoptotik değişiklikler

Musa DİRLİK¹, Hakan CANBAZ¹, Duygu DÜŞMEZ APA², Mehmet ÇAĞLIKÜLEKÇİ¹, Faik YAYLAK¹, Ebru BALLI³, Lülüfer TAMER⁴, Arzu KANIK⁵, Süha AYDIN¹

Departments of ¹General Surgery, ²Pathology, ³Histology, ⁴Biochemistry, and ⁵Biostatistics, Mersin University, School of Medicine, Mersin

Background/aims: We aimed to determine the progress of lipid peroxidation and ultrastructural changes established in the rat liver after acute bile duct ligation. **Methods:** Groups A1, B1, C1 and D1 were the controls of groups A2, B2, C2 and D2, which represented the 1st, 3rd, 5th and 8th days after bile duct ligation. Serum bilirubin and malondialdehyde, liver malondialdehyde and reduced glutathione levels, and inducible nitric oxide synthase expression were determined. Liver tissue was examined with light and electron microscopy. **Results:** Serum bilirubin increased progressively. Serum and liver malondialdehyde and inducible nitric oxide synthase expression reached a peak level at day 3, reduced at the 5th day and continued at a constant rate. Reduced glutathione decreased progressively. Ductal proliferation increased progressively to a plateau at day 5. The marked electron microscopic changes were detected at day 3 (B2) and continued constantly. **Conclusions:** The first five days after acute bile duct ligation are the most critical.

Key words: Cholestasis, lipid peroxidation, reduced glutathione, inducible nitric oxide synthase, apoptosis, ultrastructure

INTRODUCTION

Obstructive jaundice (OJ) occurs in many clinical conditions like gallstone, benign stricture or tumor of the bile duct, and complications of biliary surgery or pancreatitis, and may lead to serious complications like wound breakdown, sepsis, coagulopathy, gastrointestinal hemorrhage, cardiovascular problems, immune depression, and hepatic and renal failure (1).

The mechanisms and mediators responsible for the pathogenesis of liver damage from acute biliary obstruction remain largely unknown, although intrahepatic accumulation of toxic bile salts is tho-

Amaç: Bu çalışmada safra yolu bağlanan sıçanlarda zamana bağlı olarak lipid peroksidasyonu ve karaciğer hücrelerinde oluşan elektron mikroskopik değişikliklerin değerlendirilmesini amaçladık. **Yöntem:** A1, B1, C1 ve D1 grupları A2, B2, C2 ve D2 gruplarının kontrol grupları olup sırasıyla safra yolu bağlanması sonrası birinci, üçüncü, beşinci ve sekizinci günlere ait örneklerdir. Serum bilirubin ve malondialdehid, karaciğer malondialdehid ve redükte glutathione, indüklenebilir nitrik oksid sentaz ekspresyonu ölçüldü. Karaciğer dokusu elektron mikroskopu ile incelendi. **Bulgular:** Serum bilirubin sürekli olarak yükseldi. Serum ve karaciğer malondialdehid, ve indüklenebilir nitrik oksid sentaz ekspresyonu üçüncü gün en yüksek seviyeye ulaştı, beşinci gün azaldı ve sabit bir değerde devam etti. Redükte glutathione değeri sürekli azaldı. Ductal proliferasyon sürekli artarak beşinci gün plato oluşturdu. Belirgin elektron mikroskopik değişiklikler üçüncü gün (B2) görüldü ve aynı şekilde devam etti. **Sonuç:** Akut safra yolu bağlanmasından sonraki ilk beş gün en kritik günlerdir.

Anahtar kelimeler: Kolestaz, lipid peroksidasyonu, redükte glutathione, indüklenebilir nitrik oksid sentaz, apoptosiz, elektron mikroskopik değişiklikler

ught to be one of the important causes (2, 3). Increased production of proinflammatory cytokines, such as tumor necrosis factor- α (TNF- α), interleukin-1beta (IL-1 β) and IL-6, has also been implicated (4). Other data suggest that additional important factors include bacterial endotoxins (5-8) and oxidative stress (6).

Lipid peroxidation, nitric oxide formation and increased expression of inducible nitric oxide synthase (iNOS) take place in hyperbilirubinemia (9). The anti-oxidant defense system is impaired by decrease in reduced glutathione (GSH) and the

activity of glutathione peroxidase in OJ. Moreover, the severity of jaundice correlates with high lipid peroxide levels and low anti-oxidant levels (10). The expression of iNOS can be regulated at the level of transcription, and nuclear factor kappa B (NF- κ B) activation is essential for its expression (11). NF- κ B activates endogenous iNOS via IKK, and provides protection from apoptosis (12).

The systemic consequences of hyperbilirubinemia and OJ are well known, and the literature describes that there is a competition between apoptotic and anti-apoptotic processes in liver tissue after the initial insult. We think that while this competition may be exaggerated, complex and chaotic in the beginning, as the insult persists, the rate of apoptosis later reaches a continuous constant rate. This is a complex process and there is insufficient information in the literature about the monitoring of mediators responsible in liver injury. We thus designed a time-dependent study with acute bile duct-ligated rats to determine the progress in lipid peroxidation and apoptosis of liver cells by monitoring the rate of lipid peroxidation, anti-oxidative capacity, iNOS expression, and ultrastructural changes in a time-dependent manner.

MATERIALS AND METHODS

After the approval of the ethics committee (date and number of approval: October 04, 2004-14/2) of the Institution, 56 male, Wistar rats, weighing 250-300 g, were housed at constant temperature with 14/10 hour (h) periods of light and dark exposure, respectively. Animals were allowed access to standard rat chow and water *ad libitum* during an acclimation period of at least five days prior to use in experiments. Experiments were performed in the Animal Experimental Laboratory of the Institution in adherence to the National Institutes of Health guidelines on the use of experimental animals.

We randomized 56 rats into 8 groups as follows:

Group A1: Control group of 1st day; (n=6).

Group A2: 1st day after bile duct ligation (BDL); (n=8).

Group B1: Control group of 3rd day; (n=6).

Group B2: 3rd day after BDL; (n=8).

Group C1: Control group of 5th day; (n=6).

Group C2: 5th day after BDL; (n=8).

Group D1: Control group of 8th day; (n=6).

Group D2: 8th day after BDL; (n=8).

Surgical Procedures

Rats were anesthetized with intramuscular ketamine 50 mg kg⁻¹ and xylazine 7 mg kg⁻¹. The abdomen was cleaned with 1% polyvinyl iodine and median laparotomy was performed. The experimental jaundice was created by ligation of the common bile duct as described by Lee (13). Bile ducts of the rats in each control group were dissected, but not ligated. Rats in groups A1/A2, B1/B2, C1/C2, and D1/D2 were sacrificed at the end of the 1st, 3rd, 5th and 8th days, respectively. Prior to sacrifice, rats were anesthetized with intramuscular ketamine (50 mg kg⁻¹) and blood was taken by cardiac puncture just prior to total hepatectomy through a midline incision.

Direct bilirubin, malondialdehyde (MDA) levels of serum and MDA and GSH levels of liver tissue were detected using biochemical methods. Liver tissue samples were harvested in order to evaluate ultrastructural changes with electron microscopy, for histopathological examination with light microscopy, and to determine liver tissue iNOS expression. The liver tissue iNOS expression was illustrated immunohistopathologically. The pathologist was blinded to group allocations.

Biochemical Analysis

Serum bilirubin determination

The direct bilirubin levels were analyzed by Cobas Integra 700 biochemical analyzer (Roche Diagnostics, GmbH, Mannheim, Germany).

Lipid Peroxides Assays

Serum and tissue MDA determination

The MDA levels, as an index of lipid peroxidation, were determined by thiobarbituric acid (TBA) reaction according to Yagi. The principle of the method depends on spectrophotometric measurement of the pink color produced by interaction of the barbituric acid with MDA elaborated as a result of lipid peroxidation. The colored reaction 1, 1, 3, 3 tetraethoxypropane was used as the primary standard at 553 nm (14).

Tissue GSH determination

After liver tissue was homogenized in 5% NaCl, GSH, an index of the anti-oxidant defense system, was measured according to the Srivastava and Beutler (15). The principle of the test is based on the 5,5' Dithiobis (2-nitro benzoic acid) [DTND], which is a disulfide compound that is readily reduced by

sulfhydryl compounds, forming a highly colored yellow anion. The optical density of this yellow substance is measured at 412 nm.

Histopathology

The extracted liver tissue was fixed in 10% phosphate-buffered formaldehyde solution and subsequently embedded in paraffin, sectioned, and finally stained with hematoxylin and eosin (H-E). The following scoring system of ductal proliferation, actually defined for determination of severity of obstructive cholangitis, was used:

- 0: <10% of portal areas involved;
- 1: 10-50% of portal areas involved;
- 2: >50% of portal areas involved;
- 3: Circumferential involvement of at least 50% of the portal areas without significant expansion of the portal tract;
- 4: Circumferential involvement of at least 50% of the portal areas with significant expansion of the portal tract;
- 5: Same as 4 plus bridging of the portal tracts in <20% of instances;
- 6: Same as 4 plus >20% of the portal tracts showing bridging involvement.

Immunohistochemistry

Inducible NOS expression was detected to evaluate intensity of lipid peroxidation and hepatocyte apoptosis. iNOS staining was quantified in paraffin-embedded sections. 5 μ m sections were obtained and stained with avidin-biotin complex immunoperoxidase. iNOS was observed in the cytoplasm of liver parenchyma cells. Primary antibodies used were rabbit anti-iNOS, a synthetic peptide derived from the extreme C-terminus of the human iNOS protein (Zymed Laboratories, San Francisco, CA, USA), with a dilution of 1:1000. The sections were deparaffinized in xylene through ethanol to phosphate-buffered saline (PBS; pH 7.2). 3% hydrogen peroxide was applied for 30 minutes (min) to inhibit endogenous peroxidase activity. The slides incubated in citrate buffer were heated in a microwave oven for 5 min. Twenty minutes later, they were removed and ultra V block (Labvision, Fremont, CA, USA) was added. Primary antibody for iNOS was added and the slides were incubated for one night in a moist chamber at 4° C. Subsequently, they were incubated in biotinylated goat anti-polyvalent (Labvision, Fremont, CA, USA) for 10 min and in streptavidin pe-

roxidase (Labvision, Fremont, CA, USA) for 20 min. Finally, the slides were treated with AEC substrate system (Labvision, Fremont, CA, USA) for about 3 min. The sections were rinsed with distilled water and tap water after incubation periods. The tissue was counterstained with Mayer's hematoxylin. All slides were covered with a cover slip after they were fixed in buffered glycerine.

Morphometric Determination

Inducible NOS expression was scored based on extent of staining in the parenchyma cells of liver tissue under the microscope: (0) < 2% -no staining, (1) 2-10% -weak staining-, (2) 10-50% -intermediate staining-, and (3) >50% -strong staining-. The pattern of staining in pericentral or periportal areas was also noted.

Electron Microscopy

Liver tissues were fixed with 2.5% glutaraldehyde, post-fixed with 1% osmium tetroxide, dehydrated in graded alcohol series, cleared with propylene oxide, and embedded in Spurr resin (Cat No: 14300, EMS). Thin sections (50-70 nm) were cut by Leica UCT-125 and contrasted with uranyl acetate and lead citrate. Sections were examined and photographed by JEOL JEM-1011 electron microscope.

During electron microscopic examination, peripheral chromatin condensation in the nucleus and irregular shape of the nucleus were considered as apoptotic nuclear changes. Peripheral chromatin condensation is one of the most important findings of the apoptosis.

Statistical Analysis

Biochemical values were described as mean \pm standard deviation (SD). Statistical differences for serum direct bilirubin, serum and tissue MDA and tissue GSH values were evaluated using one-way ANOVA followed by Tukey HSD *post hoc* test SPSS version 11.5 (SPSS Inc., Chicago, IL, USA). Histopathological examinations were presented as median with 25th to 75th percentiles. Comparisons of iNOS staining scores and ductal proliferation scores (DPSs) were analyzed using Kruskal-Wallis test followed by Dunn test (Statistica 6.1, Statsoft, Inc.). P values less than 0.05 were considered statistically significant. Error bar graphics were used to show mean \pm 95% confidence interval of biochemical values. Box-plot graphics were used to show medians of histopathological scores.

Table 1. The results of evaluation parameters in all groups

	A1	A2	B1	B2	C1	C2	D1	D2
Direct Bilirubin[†] (mg/dl)	0.37±0.04	4.96±1.21	0.40±0.02	12.74±1.83	0.34±0.01	15.66±1.10	0.33±0.01	17.78±1.83
MDA[†] (nmol/ml)	7.15±0.92	17.67±7.64	9.42±3.22	56.12±13.21	6.12±1.24	28.27±5.58	6.35±0.78	29.51±8.47
MDA[‡] (nmol/g)	7.90±1.09	21.63±4.29	9.27±0.27	24.56±8.90	8.48±1.80	23.86±3.03	9.59±1.94	20.00±2.31
Reduced GSH[‡] (mg/dl)	2.92±0.52	1.89±0.57	3.10±0.01	1.41±0.14	3.07±0.01	1.29±0.21	2.81±0.34	1.15±0.11

Biochemical values in each group were described as mean ± standard deviation.

[†]: Serum. [‡]: Liver. MDA: Malondialdehyde. GSH: Glutathione.

Table 2. Ductal proliferation and immunohistochemical iNOS expression scores

	A1	A2	B1	B2	C1	C2	D1	D2
Liver ductal proliferation	0 [0-0]	1 [1-1]	0 [0-0]	2 [2-2]	0 [0-0]	4 [4-5]	0 [0-0]	4 [4-4.25]
Liver iNOS	0 [0-0]	0 [0-1]	0 [0-0]	2 [1.75-2.25]	0 [0-0]	1.5 [1-2.25]	0 [0-0]	0 [0-2.25]

Value of each group was described as median with [25th- 75th] percentiles.

RESULTS

Biochemical Analysis

The results of all biochemical values are presented as mean ± standard deviation (SD) in Table 1.

Serum bilirubin

Serum direct bilirubin levels of each BDL group were significantly higher than those of the accompanying control groups ($p < 0.05$ for each comparison). Serum direct bilirubin levels of groups B2, C2 and D2 were significantly higher than of group A2, and values of groups C2 and D2 were significantly higher than of group B2 ($p < 0.05$ for each comparison) (Figure 1). The level of direct bilirubin increased progressively as the duration of BDL increased.

Serum and tissue MDA

Serum and liver MDA levels of each OJ group were significantly higher than those of the accom-

panying control groups ($p < 0.05$ for each comparison). Serum MDA level of group B2 was significantly higher than of groups A2, C2 and D2 ($p < 0.05$ for each comparison). When the liver MDA levels of BDL groups were compared, there was no significant difference between these groups ($p > 0.05$ for each comparison) (Figure 2).

The increment in levels of serum and tissue MDA started after BDL and reached a significant value at the end of the 1st day. When BDL groups were compared, serum MDA reached a significantly high peak value on the 3rd day and then decreased significantly. Liver MDA reached a peak value on the 3rd day and then decreased thereafter, but these variations were not significant.

Tissue GSH

Liver GSH level of each BDL group was significantly lower than its control group ($p < 0.005$ for each comparison). Liver GSH level of group A2 was significantly higher than of groups B2, C2 and D2 ($p < 0.05$ for each comparison) (Figure 3).

Bile duct ligation caused a significant decrease in liver GSH level starting from the 1st day. When OJ groups were compared, this decrement was significant on the 3rd and following days; however, this decline slowed after the 3rd day.

Histopathology

The results of all histopathological examinations are presented in Table 2 as median with 25th to 75th percentiles.

The portal tract histopathological changes after BDL were: bile duct proliferation, portal tract edema, neutrophilic inflammation, and cholestasis of periportal hepatocytes, and there was necrosis in some of the cases. Figure 4A shows representative

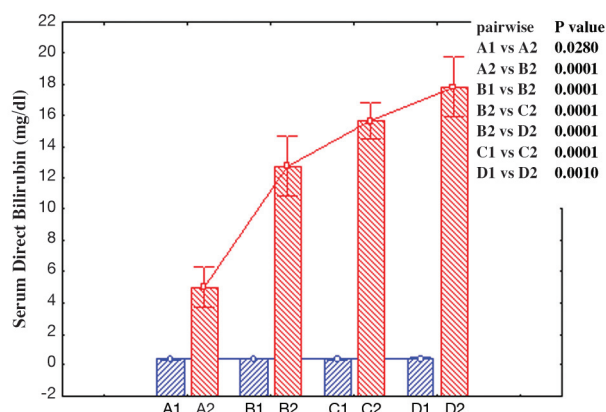


Figure 1. The error bar graphs with the mean and 95% confidence intervals and the significance levels of pairwise comparisons of serum direct bilirubin.

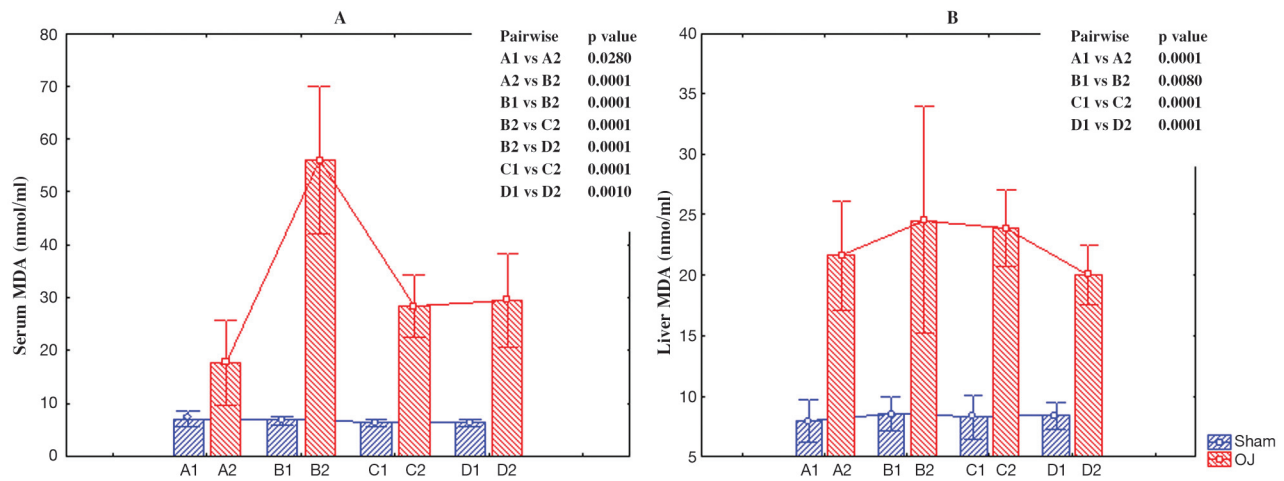


Figure 2. The error bar graphs with the mean and 95% confidence intervals and the significance levels of pairwise comparisons of serum MDA (A) and liver MDA (B).

portal tract histopathological changes after BDL. DPS of each BDL group was significantly higher than the accompanying control group ($p < 0.05$ for each comparison). DPSs of groups B2, C2 and D2 were significantly higher than of group A2, and values of groups C2 and D2 were higher than of group B2 (Figure 5A).

Histopathological changes after BDL were not observed in the control groups (groups A1, B1, C1 and D1). Histopathological changes increased progressively from group A2 to group C2, in which they reached a plateau. When BDL groups were compared, the changes significantly progressed until the 5th day of BDL and did not change thereafter.

Immunohistochemistry

No iNOS expression was seen in the control groups (A1, B1, C1 and D1) or group A2. In group B2, there was a strong cytoplasmic iNOS staining located mostly in the pericentral area of the liver lobules. In groups C2 and D2, iNOS expression was intermediate to strong. Figure 4B shows representative strong iNOS staining in the immunohistochemical examination of liver tissue. Except for group A2, iNOS expression in the BDL groups was significantly higher than in the accompanying control groups ($p < 0.005$ for each comparison). iNOS expression in groups B2 and C2 was significantly higher than in A2 ($p < 0.005$ for each comparison) (Figure 5B).

Bile duct ligation caused a significant increase in iNOS staining starting from the 3rd day of BDL. When BDL groups were compared, iNOS staining

significantly increased and reached a peak level on the 3rd day after BDL and then decreased on day 5, but the decline was not significant when compared with the 3rd day of BDL.

Ultrastructural Changes in Electron Microscopic Examination

Groups A1, B1, C1 and D1: Normal hepatocyte, bile canaliculi, bile duct, sinusoid and Disse space structures were seen (Figure 6).

Group A2: Although normal bile canaliculi structure was observed, some structural changes were detected in cells of bile ducts including apoptotic nuclear changes, dilatation of rough endoplasmic reticulum (RER) cistern and perinuclear cistern, and myelin figures in the cytoplasm. Moreover, ac-

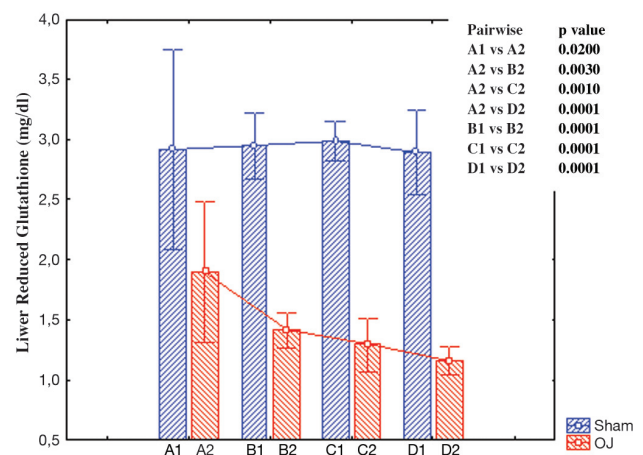


Figure 3. The error bar graphs with the mean and 95% confidence intervals and the significance levels of pairwise comparisons of liver reduced glutathione.

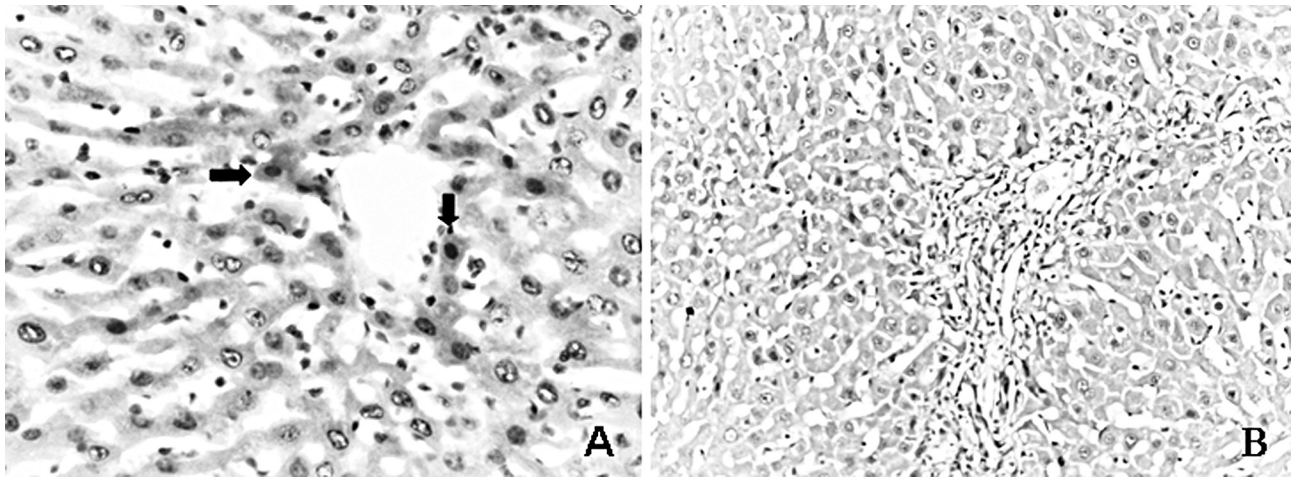


Figure 4. Representative portal tract histopathological changes of obstructive cholestasis in the liver tissue. Hematoxylin-eosin (H-E) x200 (A), representative strong iNOS staining (arrow) in the immunohistochemical examination of liver tissue, X400 (B).

cumulation of some wasted material was detected in the lumen of the bile duct. Mitochondrial swelling, diffuse dilatation of RER and perinuclear cistern, and nuclear apoptotic changes were observed in hepatocytes.

Group B2: Dilatation of bile canaliculi, hepatocyte surface disorganization and irregular microvilli were observed. Some wasted material accumulation was seen in the lumen of the bile canaliculi (Figure 7A, 7B and 7C). Structural abnormalities of the bile duct, which had been detected in day 1, were also observed on the 3rd day (Figure 7D). Mitochondrial degenerative findings and dilatation of RER and perinuclear cistern of hepatocytes were

re determined (Figure 7A, 7B and 7C).

Group C2: Prominent dilatation of bile canaliculi, irregular microvilli and loss of microvilli were easily detected on this day. In addition, bile duct abnormalities became more evident. Defects observed in hepatocytes continued.

Group D2: The findings observed in groups B2 and C2 were also detected in this group.

Normal bile canaliculi structure was seen in the control groups. Apoptotic nuclear changes, dilatation of RER cistern and perinuclear cistern, and degenerative mitochondrial changes in the cells of bile ducts and hepatocytes were detected from day 1. Dilatation of bile canaliculi, hepatocyte surface

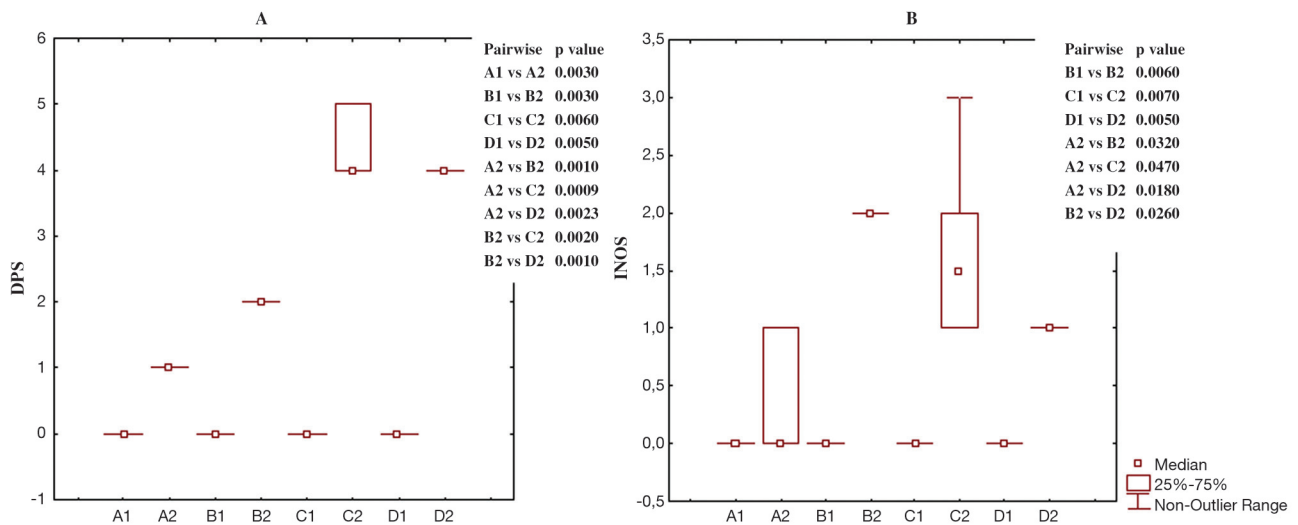


Figure 5. The differences and multiple comparisons between medians of liver ductal proliferation values (A) and immunohistochemical examination of liver tissue iNOS staining values (B) of each group in the histopathological examination with light microscopy, with box-plot graphics.

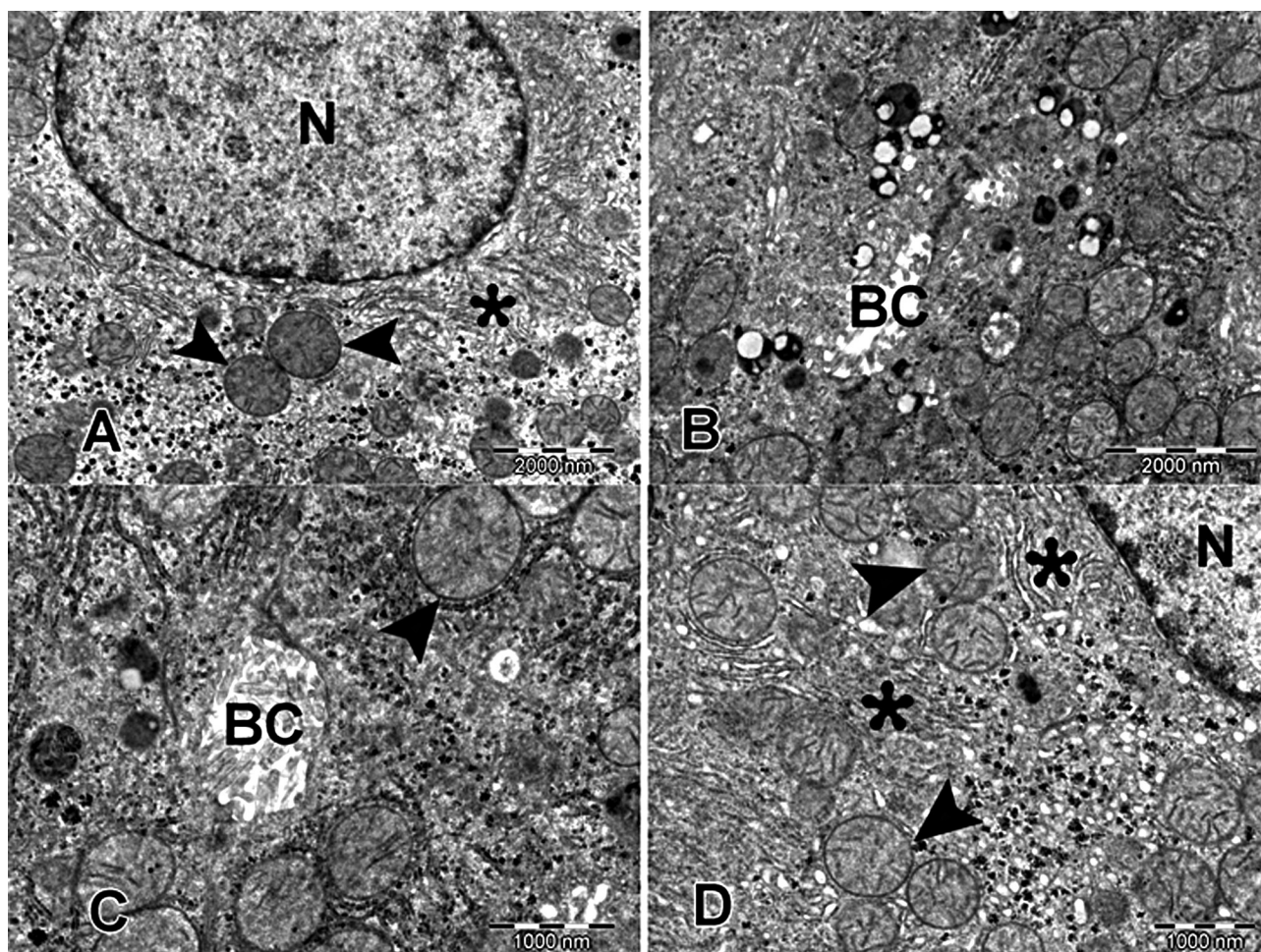


Figure 6. Electron microscopic appearance of liver tissue of control groups (A1, B1, C1 and D1). **A:** Day 1: Normal hepatocyte. Nucleus (N), rough endoplasmic reticulum (asterisk) and mitochondria (arrowhead). **B:** Day 3: Normal bile canaliculi (BC) structure. **C:** Day 5: Normal BC and mitochondria (arrowhead). **D:** Day 8: Normal hepatocyte. Nucleus (N), rough endoplasmic reticulum (asterisk) and mitochondria (arrowhead).

disorganization and irregular microvilli were observed on day 3. All of these findings were markedly established on day 3. Defects observed in the cells of bile ducts and hepatocytes continued constantly from day 3 to day 8.

DISCUSSION

Bile acids are accumulated in cholestasis (16) and induce hepatocyte apoptosis and necrosis (17). Bile acids and toxic bile salts like glycochenodeoxycholate (GCDC) cause oxidative damage to cell membranes by stimulating the oxygen free radicals from mitochondria (18).

The anti-oxidant defense system is impaired by decrease in GSH and the activity of glutathione peroxidase in hyperbilirubinemia. Moreover, the severity of hyperbilirubinemia correlates with high lipid peroxide levels and low anti-oxidant le-

vels (10). Exaggerated lipid peroxidation, oxidative stress and accumulation of toxic hydrophobic bile salts within hepatocytes in jaundiced rats cause hepatocyte toxicity, which leads to liver damage. MDA has been used as an index of lipid peroxidation in the literature. In our experimental study, we observed that serum and liver MDA started to increase on day 1, reached a peak value on the 3rd day and decreased on the 5th and 8th days of BDL. There was no difference in serum and liver MDA levels between the 5th and 8th days of BDL, even though direct bilirubin levels continued to increase. This shows that there is an exaggerated increase in lipid peroxidation within the first five days after BLD. On the 5th day, rate and intensity of lipid peroxidation had stabilized and reached a continuous constant rate. This fact is not dependent on the level of direct bilirubin; although the duration of BDL is increased, there is

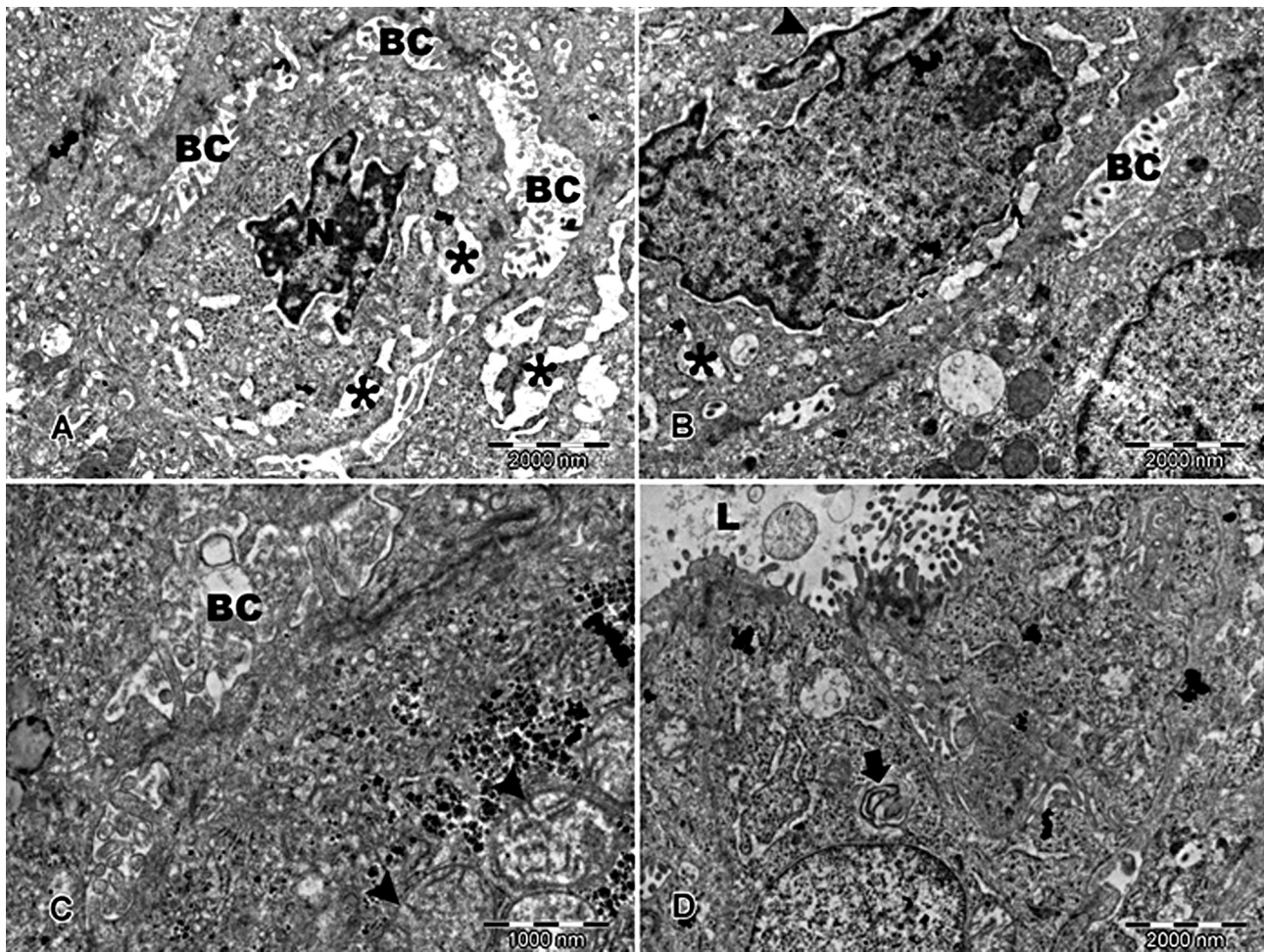


Figure 7. Electron microscopic appearance of liver tissue on the third day after bile duct ligation (Group B2). **A:** Bile canaliculi (BC), hepatocyte nucleus (N) and dilate rough endoplasmic reticulum cisternae (asterisk). **B:** BC, dilated rough endoplasmic reticulum (asterisk) and perinuclear cisternae (arrowhead). **C:** BC and mitochondria (arrowhead). **D:** Bile duct. Myelin figure (arrow) in duct cell cytoplasm and lumen (L).

an insignificant reduction in lipid peroxidation.

On the other hand, we observed that there was a continuous reduction in GSH levels. The continuous reduction in GSH levels shows that there is a continuous reduction in anti-oxidative capacity as long as the duration of BDL increased. The marked reduction was detected on the 3rd and 5th days of BDL, and this decline slowed after the 3rd day. This fact shows that anti-oxidative capacity had stabilized and reached a continuous constant rate on the 5th day after BDL.

In inflammatory conditions, hepatocyte survival is dependent on the protective function of anti-apoptotic genes (19) and iNOS, which have been identified to have anti-apoptotic roles in mature hepatocytes by controlling the transcription of specific survival genes (20, 21). NF- κ B is the prototypic transcription factor in eukaryotic cells known to

play a pivotal role in transactivation of promoters for genes involved in inflammation, immune responses, and the anti-apoptotic mechanism (22).

Nitric oxide inhibits caspase-3 activity in hepatocytes (23). NO production depends on the expression of iNOS in response to inflammatory cytokines (24, 25). It is known that iNOS gene transfer could suppress hepatocyte apoptosis (26). iNOS is heterogeneously distributed in the liver (27, 28), which may represent a mechanism through which hepatocytes control the degree of apoptosis in the liver (29, 30). In present study, BDL caused a significant increase in iNOS staining on the 3rd day. iNOS staining significantly increased and reached a peak level on the 3rd day after BDL and then decreased on the 5th day, but the decline was not significant when compared with the 3rd day of BDL. Normally, GSH up-regulates NO

synthesis via increasing iNOS mRNA levels and iNOS activity (31). The reduction in GSH level leads to the reduction in iNOS protein and NO synthesis on the 5th day of BDL.

The severity of cholestasis can be evaluated by examining and scoring the ductal proliferation in the liver tissue with light microscopy. Cholestatic histopathological changes were not observed in the control groups. The cholestatic changes progressively increased throughout the 1st, 3rd and 5th days of BDL and reached a plateau on the 5th day, and remained unchanged on the 8th day. This data shows that cholestatic histopathological changes depend upon lipid peroxidation, oxidative stress and accumulation of toxic hydrophobic bile salts within hepatocytes. High iNOS production suppresses hepatocyte apoptosis. Low iNOS expression and retention and accumulation of toxic hydrophobic bile salts within hepatocytes aggravate hepatocyte apoptosis. Reduction in GSH level leads to down-regulation of iNOS expression and alleviates the suppressor effect of iNOS on hepatocyte apoptosis. Apoptotic and anti-apoptotic processes balance the rate of hepatocyte apoptosis. Thus, cholestatic histopathological changes reached a plateau on the 5th day when the down-regulation of iNOS expression was established.

Ultrastructural changes in the electron microscopic examination of liver tissue showed that apoptotic changes in the cells of bile ducts and hepatocytes depended upon the severity of lipid peroxidation, tissue GSH levels (anti-oxidant capacity) and anti-apoptotic effect of iNOS. In electron microscopic examination, minimal apoptotic changes were detected on day 1. All of these findings were markedly established on day 3. Defects observed in the cells of bile ducts and hepatocytes continu-

ed constantly from day 3 to day 8. As the duration of hyperbilirubinemia progressed, these findings continued constantly. The hepatocyte control on the degree of apoptosis was depressed, because the reduction in GSH level led to down-regulation of iNOS protein and NO synthesis. There was a competition between apoptotic forces (cholestasis and lipid peroxidation) and anti-apoptotic genes and iNOS. Down-regulation of iNOS protein and NO synthesis led to more evident apoptotic changes detected on the 3rd, 5th and 8th days of BDL.

CONCLUSIONS

1. Lipid peroxidation and anti-oxidative capacity had stabilized and reached a continuous constant rate on the 5th day after BDL.
2. iNOS production had stabilized and reached a continuous constant rate on the 5th day after BDL.
3. Cholestatic histopathological changes had stabilized and reached a continuous constant rate on the 5th day after BDL.
4. Apoptotic changes in the cells of bile ducts and hepatocytes were markedly established on day 3 and continued constantly from day 3 to day 8.

Although apoptotic changes in hepatocytes were markedly established on day 3, other findings had stabilized and reached a continuous constant rate on the 5th day after BDL. We thus can state that cholestatic liver injury is established and becomes obvious on the 5th day after acute BDL. Thus, we recommend testing the protective effect of anti-apoptotic agents, anti-oxidants and iNOS inhibitors on cholestatic liver injury before the 5th day and testing the therapeutic effect of these agents after the 5th day.

REFERENCES

1. Greig JD, Krukowski ZH, Matheson NA. Surgical morbidity and mortality in one hundred and twenty-nine patients with obstructive jaundice. *Br J Surg* 1988; 75: 216-9.
2. Miyoshi H, Rust C, Roberts PJ, et al. Hepatocyte apoptosis after bile duct ligation in the mouse involves Fas. *Gastroenterology* 1999; 117: 669-77.
3. Miyoshi H, Rust C, Guicciardi ME, Gores GJ. NF-kappaB is activated in cholestasis and functions to reduce liver injury. *Am J Pathol* 2001; 158: 967-75.
4. Lechner AJ, Velasquez A, Knudsen KR, et al. Cholestatic liver injury increases circulating TNF-alpha and IL-6 and mortality after *Escherichia coli* endotoxemia. *Am J Respir Crit Care Med* 1998; 157: 1550-8.
5. Moazzam FN, Brems JJ, Yong SL, et al. Endotoxin potentiates hepatocyte apoptosis in cholestasis. *J Am Coll Surg* 2002; 194: 731-9.
6. Liu TZ, Lee KT, Chern CL, et al. Free radical-triggered hepatic injury of experimental obstructive jaundice of rats involves overproduction of proinflammatory cytokines and enhanced activation of nuclear factor kappaB. *Ann Clin Lab Sci* 2001; 31: 383-90.
7. Ito Y, Machen NW, Urbaschek R, McCuskey RS. Biliary obstruction exacerbates the hepatic microvascular inflammatory response to endotoxin. *Shock* 2000; 14: 599-604.
8. Houdijk AP, van Lambalgen AA, Thijs LG, Van Leeuwen PA. Gut endotoxin restriction improves postoperative hemodynamics in the bile duct-ligated rat. *Shock* 1998; 9: 282-8.
9. Arriero MM, Lopez-Farre A, Fryeiro O, et al. Expression of inducible nitric oxide synthase in the liver of bile duct-ligated Wistar rats with modulation by lymphomononuclear cells. *Surgery* 2001; 129: 255-66.

10. Holt S, Marley R, Fernando B, et al. Acute cholestasis-induced renal failure: effects of antioxidants and ligands for the thromboxane A2 receptor. *Kidney Int* 1999; 55: 271-7.
11. Xie QW, Kashiwabara Y, Nathan C. Role of transcription factor NF-kappa B/Rel in induction of nitric oxide synthase. *J Biol Chem* 1994; 269: 4705-8.
12. Hatano E, Bennett BL, Manning AM, et al. NF-kappaB stimulates inducible nitric oxide synthase to protect mouse hepatocytes from TNF-alpha- and Fas-mediated apoptosis. *Gastroenterology* 2001; 120: 1251-62.
13. Lee E. The effect of obstructive jaundice on the migration of reticulo-endothelial cells and fibroblasts into early experimental granulomata. *Br J Surg* 1972; 59: 875-7.
14. Yagi K. Lipid peroxides and related radicals in clinical medicine. In: Armstrong D, ed. *Free radicals in diagnostic medicine*. New York: Plenum Press, 1994; 1-15.
15. Lowry OH, Roscrough NJ, Farr AI, Randat RJ. Protein measurement with the folin phenol reagent. *J Biol Chem* 1954; 193: 265-75.
16. Lauterburg BH, Dickson ER, Pineda AA, Taswell HF. Depletion of bile acids and bilirubin in dogs with biliary obstruction by plasma perfusion of USP-charcoal-coated glass beads. *Int J Artif Organs* 1980; 3: 281-5.
17. Hofmann AF. Cholestatic liver disease: pathophysiology and therapeutic options. *Liver* 2002; 22: 14-9.
18. Bomzon A, Holt S, Moore K. Bile acids, oxidative stress, and renal function in biliary obstruction. *Semin Nephrol* 1997; 17: 549-62.
19. Schoemaker MH, Ros JE, Homan M, et al. Cytokine regulation of pro- and anti-apoptotic genes in rat hepatocytes: NF-kappaB-regulated inhibitor of apoptosis protein 2 (cIAP2) prevents apoptosis. *J Hepatol* 2002; 36: 742-50.
20. LaCasse EC, Baird S, Korneluk RG, MacKenzie AE. The inhibitors of apoptosis (IAPs) and their emerging role in cancer. *Oncogene* 1998; 17: 3247-59.
21. Wang K, Brems JJ, Gamelli RL, Ding J. Reversibility of caspase activation and its role during glycochenodeoxycholate-induced hepatocyte apoptosis. *J Biol Chem* 2005; 280: 23490-5.
22. Xiong S, She H, Takeuchi H, et al. Signaling role of intracellular iron in NF-kappaB activation. *J Biol Chem* 2003; 278: 17646-54.
23. Schoemaker MH, Gommans WM, Conde de la Rosa L, et al. Resistance of rat hepatocytes against bile acid-induced apoptosis in cholestatic liver injury is due to nuclear factor-kappa B activation. *J Hepatol* 2003; 39: 153-61.
24. Kim YM, de Vera ME, Watkins SC, Billiar TR. Nitric oxide protects cultured rat hepatocytes from tumor necrosis factor-alpha-induced apoptosis by inducing heat shock protein 70 expression. *J Biol Chem* 1997; 272: 1402-11.
25. Kim YM, Son K, Hong SJ, et al. Inhibition of protein synthesis by nitric oxide correlates with cytostatic activity: nitric oxide induces phosphorylation of initiation factor eIF-2 alpha. *Mol Med* 1998; 4: 179-90.
26. Tzeng E, Billiar TR, Williams DL, et al. Adenovirus-mediated inducible nitric oxide synthase gene transfer inhibits hepatocyte apoptosis. *Surgery* 1998; 124: 278-83.
27. Geller DA, Lowenstein CJ, Shapiro RA, et al. Molecular cloning and expression of inducible nitric oxide synthase from human hepatocytes. *Proc Natl Acad Sci U S A* 1993; 90: 3491-5.
28. McNaughton L, Puttagunta L, Martinez-Cuesta MA, et al. Distribution of nitric oxide synthase in normal and cirrhotic human liver. *Proc Natl Acad Sci U S A* 2002; 99: 17161-6.
29. de Belder AJ, Radomski MW. Nitric oxide in the clinical arena. *J Hypertens* 1994; 12: 617-24.
30. Li J, Billiar TR. Nitric oxide. IV. Determinants of nitric oxide protection and toxicity in liver. *Am J Physiol* 1999; 276(5 Pt 1): G1069-G1073.
31. Baron V, Hernandez J, Noyola M, et al. Nitric oxide and inducible nitric oxide synthase expression are down regulated in acute cholestasis in the rat accompanied by liver ischemia. *Comp Biochem Physiol C Toxicol Pharmacol* 2000; 127: 243-9.